

Inclusive strange particle production in $e^+ e^-$ annihilation

Cello Collaboration

H.-J. Behrend, L. Criegee, J.H. Field¹, G. Franke, H. Jung², J. Meyer, O. Podobrin, V. Schröder, G.G. Winter
Deutsches Elektronen-Synchrotron, DESY, Hamburg, Federal Republic of Germany

P.J. Bussey, A.J. Campbell, D. Hendry, S.J. Lumsdon, I.O. Skillicorn
University of Glasgow, Glasgow, UK

J. Ahme, V. Blobel, W. Brehm, M. Feindt, H. Fenner, J. Harjes, J.H. Köhne, J.H. Peters, H. Spitzer
II. Institut für Experimentalphysik, Universität, Hamburg, Federal Republic of Germany

W.-D. Apel, J. Engler, G. Flügge², D.C. Fries, J. Fuster³, P. Gabriel, K. Gamberdinger⁴,
P. Grosse-Wiesmann⁵, M. Hahn, U. Hädinger, J. Hansmeyer, H. Küster⁶, H. Müller, K.H. Ranitzsch,
H. Schneider, R. Seufert
Kernforschungszentrum Karlsruhe und Universität, Karlsruhe, Federal Republic of Germany

W. de Boer, G. Buschhorn, G. Grindhammer⁵, B. Gunderson, Ch. Kiesling⁷, R. Kotthaus, H. Kroha,
D. Lüers, H. Oberlack, P. Schacht, S. Scholz, W. Wiedenmann⁸
Max Planck-Institut für Physik und Astrophysik, München, Federal Republic of Germany

M. Davier, J.F. Grivaz, J. Haissinski, V. Journé, D.W. Kim, F. Le Diberder, J.-J. Veillet
Laboratoire de l'Accélérateur Linéaire, Orsay, France

K. Blohm, R. George, M. Goldberg, O. Hamon, F. Kapusta, L. Poggioli, M. Rivoal
Laboratoire de Physique Nucléaire et des Hautes Energies, Université, Paris, France

G. d'Agostini, F. Ferrarotto, M. Iacovacci, G. Shooshtari, B. Stella
University of Rome and INFN, Rome, Italy

G. Cozzika, Y. Ducros
Centre d'Etudes Nucléaires, Saclay, France

G. Alexander, A. Beck, G. Bella, J. Grunhaus, A. Klatchko, A. Levy, C. Milstène
Tel Aviv University, Tel Aviv, Israel

Received 7 November 1989

¹ Now at Université de Genève, Switzerland

² Now at RWTH, Aachen, FRG

³ Now at Inst. de Fisica Corpuscular, Universidad de Valencia, Spain

⁴ Now at MPI für Physik und Astrophysik, München, FRG

⁵ Now at Stanford Linear Accelerator Center, USA

⁶ Now at DESY, Hamburg, FRG

⁷ Heisenberg Scholarship of Deutsche Forschungsgemeinschaft

⁸ Now at CERN

Abstract. We present an analysis of strange particle production from $e^+ e^-$ annihilation into multihadronic final states. The experiment was performed with the CELLO detector at the PETRA storage ring at DESY, the data was taken at a centre of mass energy of 35 GeV with an integrated luminosity of 86 pb^{-1} . The particles K_S^0 , $K^{*\pm}$ and Λ have been identified by their characteristic decays, and differential cross sections for their pro-

duction have been obtained. From a comparison of K_S^0 and $K^{*\pm}$ rates the Lund vector meson suppression parameter $V/(V+P)_S$ has been determined.

1 Introduction

Electron positron annihilation in colliding beam machines is a kinematically simple high energy process which offers unique possibilities for studying the transition of partons into observable hadrons. The centre of mass energy is almost entirely transferred initially to the partons, just a few percent being lost on average to radiative photons. The parton state, consisting of a $q\bar{q}$ pair and up to a few hard gluons, then fragments into hadrons. In principle this transition can be calculated within QCD. But, since low energy scales are involved, the perturbative approach fails. Much effort has therefore been dedicated to a phenomenological description of these transitions in the context of fragmentation models. Usually these models introduce several parameters which arise from the underlying ideas of the model, but must be determined by experiment. The models finally deliver production cross sections for various particle species which can be compared to the experimental data.

Results from CELLO on inclusive γ , π^0 and η production have been already published [1]. In this paper we give results on strange meson and strange baryon production, and compare them to the Lund string model predictions. We first present the K_S^0 and $K^{*\pm}$ production rates, from which we infer the $V/(V+P)_S$ parameter for strange quark production (Sect. 3). Λ production is examined in Sect. 4.

2 Experiment

The CELLO detector at PETRA recorded an integrated luminosity of 86 pb^{-1} in the 1986 data taking period at 35 GeV. CELLO is a multi purpose detector and has been described in detail elsewhere [2]. The present analysis relies solely on the information from the central tracking device, which is contained within a thin superconducting solenoid of 1.6 m diameter providing an axial magnetic field of 1.3 T. During 1986 the detector was equipped with nine drift and five proportional chambers with radii from 11 to 70 cm and covering 92% of the solid angle. It achieved a momentum resolution of $\sigma(p)/p = 0.02 \cdot p$ (p in GeV/c) without vertex constraint. In the forward and backward region of the detector two planes of proportional chambers perpendicular to the beam axis complete the tracking system and allow charged particle measurement within $|\cos\theta| \leq 0.98$.

To identify multihadronic events we use a standard selection procedure, described in detail in [3]. Here we briefly mention the most important criteria. These require (1) at least five charged particles; (2) at least 1 GeV neutral energy in the lead liquid argon calorimeter; (3) at least 7 GeV total energy of charged particles in the central tracking device and (4) the net charge sum to

be less than 6. With these cuts we select 24166 events. The residual background is estimated to be less than 3% and stems primarily from two-photon reactions and beam-gas interactions.

3 Strange meson production

The neutral K_S^0 meson can be detected by its in-flight decay into $\pi^+\pi^-$, its mean decay length of about 2.7 cm being sufficient to allow the reconstruction of the secondary decay vertex in many cases. To this end a V^0 search routine is applied to the reconstructed charged particle tracks. The algorithm starts with a pairing of oppositely charged particles. The two intersection points in the $x-y$ plane are calculated and the one with the smaller z difference at the crossing point is taken as the candidate V^0 vertex. In cases where no intersection is found the point of closest approach is considered as a V^0 candidate. The V^0 candidates have to pass several requirements: (1) The two tracks must be compatible with originating from a common secondary vertex within loose geometric limits; (2) The separation between primary vertex and proposed V^0 vertex in the $x-y$ plane must exceed 4 mm; (3) the z difference of the two tracks at the intersection must be less than 50 mm; (4) the tracks must not have hits between the primary and secondary vertex, except for the two innermost chambers, where noise hits may occur even on V^0 tracks. A detailed description of the algorithm can be found elsewhere [4, 5].

The position of the primary event vertex was monitored for each individual run from collinear Bhabha events and varies slowly with the running conditions of the PETRA storage ring. Due to the bunch length of about 10 cm the z coordinate of the event vertex is only roughly known and is therefore treated as a measured parameter with error in the V^0 fit.

All surviving V^0 candidates are subjected to a 3-dimensional vertex fit introducing four kinematical and geometrical constraints and one unmeasured parameter (the $x-y$ decay length). The invariant mass is calculated from the momentum vectors of the tracks at their common vertex. The fit improves V^0 mass and momentum resolution by factors of 3 and 1.7 respectively.

3.1 Analysis of K_S^0 production

To identify a clean sample of K_S^0 we start with all secondary vertex candidates as described above. The main background stems from accidental track crossings. Other sources of background are converted photons and Λ decays into $p\pi^-$, where both tracks are considered as pions. As photon conversion can only occur in matter the following cuts were applied: V^0 candidates were rejected as converted photons when their measured decay length indicated that they had passed through the beam pipe and simultaneously the invariant mass was less than $0.3 \text{ GeV}/c^2$ with both tracks being interpreted as electrons. To reduce the combinatorial background we use a combined cut in the V^0 fit probability and the decay

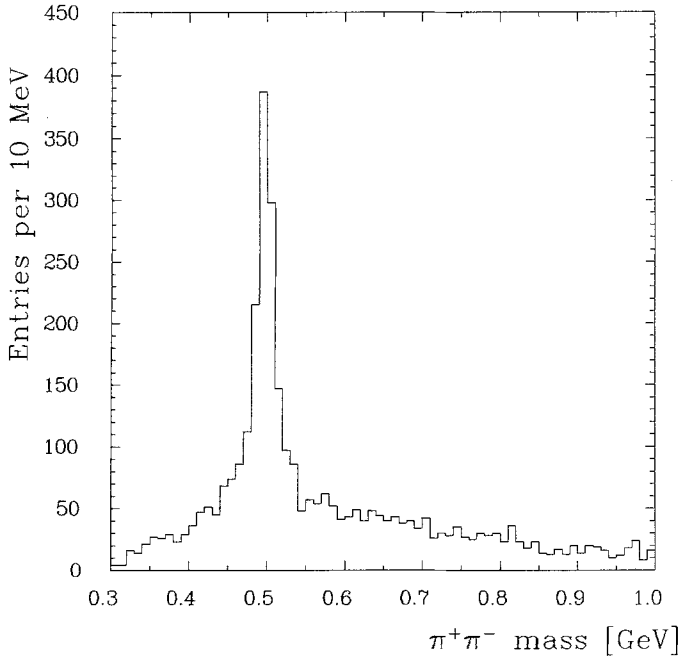


Fig. 1. $\pi^+ \pi^-$ invariant mass spectrum

Table 1. Parameters in the Lund 5.2 Monte Carlo program used for event generation

| Parameter | Value |
|-----------------------|------------------------|
| $A_{M\bar{S}}$ | 450 MeV |
| Y_{\min} | 0.015 |
| P_s | 0.3 |
| $\sigma_{p\bar{p}}$ | 250 MeV/c ² |
| $\bar{V}/(V+P)_{uds}$ | 0.4 |
| $V/(V+P)_{cb}$ | 0.75 |
| a | 1.00 |
| b | 0.60 |
| ϵ_c | 0.025 |
| ϵ_b | 0.0035 |
| $\sin^2 \theta_W$ | 0.23 |

length [5]. The resulting $\pi^+ \pi^-$ mass spectrum is shown in Fig. 1. A clear K_S^0 signal is seen above a small background. The spectrum is satisfactorily described by a polynomial background function and a Gaussian for the signal. The fit results are:

$$m(K_S^0) = 497.7 \pm 0.6 \text{ MeV}/c^2$$

and

$$\sigma(K_S^0) = 17.8 \pm 0.6 \text{ MeV}/c^2,$$

in good agreement with the PDG value and the simulated $\pi^+ \pi^-$ mass resolution. Similar fits were done in different momentum bins followed by an acceptance correction. The acceptance corrections were determined by repeating the analysis using events generated with the Lund 5.2 [6] Monte Carlo program* and passed through a detailed simulation of the CELLO detector.

* The parameters used in the Lund program are given in Table 1

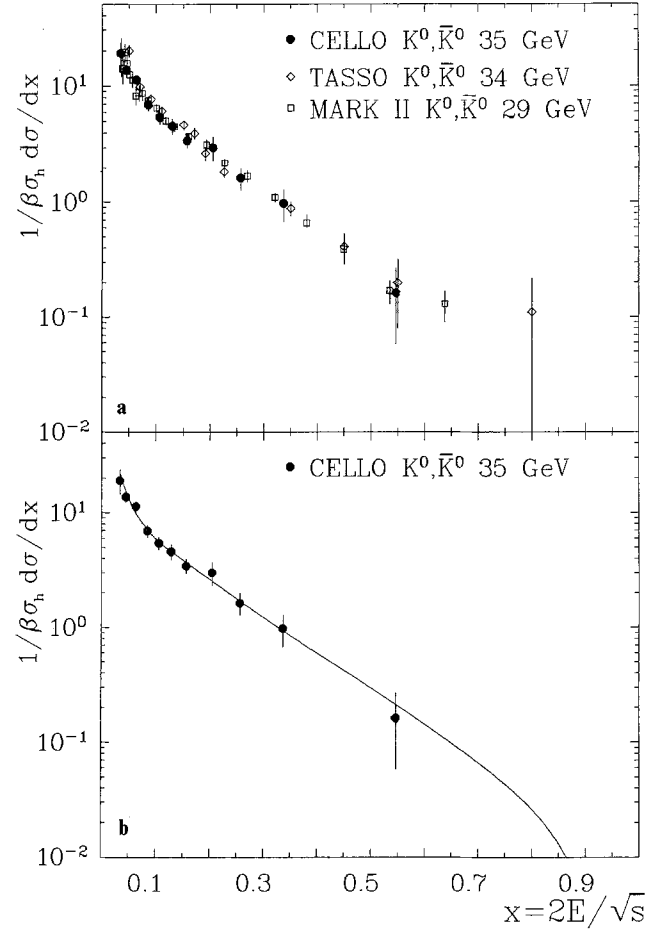


Fig. 2a, b. Scale invariant differential cross section for K^0, \bar{K}^0 production as a function of the fractional energy $x = 2E/\sqrt{s}$: a Comparison with other experiments [13, 17]; b comparison with the Lund model prediction

Table 2. K^0, \bar{K}^0 cross section. The error on the cross section is statistical only. The quoted x is the centre of gravity of the corresponding bin

| $\langle x \rangle$ | $(1/\beta\sigma_h)(d\sigma/dx)$ |
|---------------------|---------------------------------|
| 0.034 | 19.0 ± 4.46 |
| 0.045 | 13.7 ± 1.47 |
| 0.064 | 11.3 ± 1.12 |
| 0.085 | 6.95 ± 0.81 |
| 0.106 | 5.46 ± 0.70 |
| 0.129 | 4.59 ± 0.70 |
| 0.156 | 3.45 ± 0.48 |
| 0.204 | 3.01 ± 0.70 |
| 0.256 | 1.63 ± 0.35 |
| 0.337 | 0.98 ± 0.31 |
| 0.547 | 0.16 ± 0.10 |

Table 3. $K^{*\pm}$ cross section. The error on the cross section is statistical only. The quoted x is the centre of gravity of the corresponding bin

| $\langle x \rangle$ | $(1/\beta\sigma_h)(d\sigma/dx)$ |
|---------------------|---------------------------------|
| 0.125 | 3.21 ± 0.91 |
| 0.265 | 1.42 ± 0.57 |
| 0.436 | 0.24 ± 0.16 |
| 0.710 | 0.044 ± 0.039 |

Table 4. Strange particle cross sections

| Particle | Cross section [pb] | R Value | Mean multiplicity |
|------------------|-----------------------|--------------------|-----------------------|
| K^0, \bar{K}^0 | 394 ± 26 ± 51 | 5.56 ± 0.37 ± 0.72 | 1.42 ± 0.09 ± 0.18 |
| $K^{*\pm}$ | 214 ± 46 ± 39 | 3.02 ± 0.65 ± 0.54 | 0.77 ± 0.17 ± 0.14 |
| A, \bar{A} | 58.5 ± 7.6 ± 7.6 | 0.83 ± 0.11 ± 0.11 | 0.211 ± 0.027 ± 0.027 |

Table 5. A, \bar{A} cross section. The error on the cross section is statistical only. The quoted x is the centre of gravity of the corresponding bin

| $\langle x \rangle$ | $(1/\beta\sigma_h)(d\sigma/dx)$ |
|---------------------|---------------------------------|
| 0.076 | 3.25 ± 1.37 |
| 0.094 | 2.32 ± 0.49 |
| 0.117 | 1.48 ± 0.37 |
| 0.153 | 0.70 ± 0.18 |
| 0.222 | 0.32 ± 0.12 |
| 0.358 | 0.15 ± 0.07 |
| 0.585 | 0.048 ± 0.026 |

Table 6. Mean number of strange particles produced near 35 GeV from PEP and PETRA. The first error is statistical, when given the second is systematic

| Particle | Experiment | Reference | Mean multiplicity |
|------------------|------------|------------|-----------------------------------|
| K^0, \bar{K}^0 | TPC | [12] | 1.22 ± 0.03 ± 0.15 |
| | MARK II | [13] | 1.27 ± 0.03 ± 0.15 |
| | HRS | [14] | 1.58 ± 0.03 ± 0.08 |
| | PLUTO | [15] | 1.46 ± 0.3 |
| | JADE | [16] | 1.45 ± 0.08 ± 0.15 |
| | TASSO | [17] | 1.48 ± 0.05 ± 0.22 |
| | CELLO | this expt. | 1.42 ± 0.09 ± 0.18 |
| $K^{*\pm}$ | MARK II | [18] | 0.26 ± 0.047 ± 0.055 ^a |
| | HRS | [19] | 0.62 ± 0.045 ± 0.04 |
| | JADE | [20] | 0.87 ± 0.16 ± 0.08 |
| | CELLO | this expt. | 0.77 ± 0.17 ± 0.14 |
| A, \bar{A} | MARK II | [21] | 0.213 ± 0.012 ± 0.018 |
| | HRS | [14] | 0.217 ± 0.009 ± 0.022 |
| | TPC | [22] | 0.197 ± 0.012 ± 0.017 |
| | TASSO | [23] | 0.218 ± 0.011 ± 0.021 |
| | JADE | [24] | 0.234 ± 0.064 ^b |
| | CELLO | this expt. | 0.211 ± 0.027 ± 0.027 |

^a for $p > 2$ GeV/c^b The numbers given for \bar{A} only, were multiplied by two

Radiative corrections of the initial state electrons have been determined for each acceptance bin separately, using the Berends-Kleiss generator [7] implemented in the Lund Monte Carlo program. In order to check the correction procedure we measured the proper lifetime of the K_S^0 meson and found it to be in agreement with the PDG value.

The scale invariant cross section $(1/\beta\sigma_h)(d\sigma/dx)$ for inclusive K^0 and \bar{K}^0 production, expressed as a fraction

** For brevity we write just the particle state to indicate both particle and antiparticle state

of the first order hadronic cross section $\sigma_h = R_{\text{had}} \cdot \sigma(\mu^+ \mu^-)$, is presented in Table 2 as a function of the fractional energy $x = 2 \cdot E/\sqrt{s}$. The R_{had} value has been taken from a recent compilation to be 3.91 ± 0.04 at 35 GeV collision energy [10] and $\sigma(\mu^+ \mu^-)$ is the point cross section at 35 GeV. The error in R_{had} is not included in the numbers in Table 2. In Fig. 2 the results are compared to the Lund model prediction where good agreement is observed. Note, that throughout this paper all Lund curves are smoothed histograms, generated by Lund 6.3 [8] with parton shower option and default parameter values.

Integrating over the observed x range and using the Lund model to extrapolate over the unobserved x region, we obtain a K^0 and \bar{K}^0 inclusive cross section of $\sigma(K^0, \bar{K}^0) = 394 \pm 26 \pm 51$ pb. The branching ratio $K^0 \rightarrow K_S^0 \rightarrow \pi^+ \pi^-$ was taken to be 34.3% [9]. This cross section can be translated into an R value $\sigma(K^0, \bar{K}^0)/\sigma(\mu^+ \mu^-) = 5.56 \pm 0.37 \pm 0.72$. Dividing by R_{had} leads to a mean K^0, \bar{K}^0 multiplicity of $\langle N_{K^0, \bar{K}^0} \rangle = 1.42 \pm 0.09 \pm 0.18$ per event. The first error quoted is statistical and the second is systematic and reflects uncertainties inherent in the acceptance calculation and the measured luminosity, as well as uncertainties in the radiative correction applied to the data. The results are listed in Table 4, and are seen to be consistent with those from other PEP and PETRA experiments in Table 6 and Fig. 2.

3.2 Analysis of $K^{*\pm}$ production

The $K^{*\pm}$ is detected via its $K^0 \pi^+$ decay mode**, with the K^0 subsequently decaying into $\pi^+ \pi^-$. To reconstruct the $K^{*\pm}$ decay we identify K_S^0 within two standard deviations of the $\pi^+ \pi^-$ mass resolution, assign the nominal K_S^0 mass to the combination and pair it with all remaining tracks in the event. For details of the K_S^0 selection see Sect. 3.1. Since the $K^{*\pm}$ decay proceeds via the strong interaction, the additional track is required to approach the beam axis within 5 mm. To assure well measured tracks, the following cuts were imposed for the additional track: (1) $|\cos\theta| < 0.9$, where θ is the angle to the beam axis; (2) at least six hits in the central tracking system and (3) the momentum must exceed 200 MeV/c. To reduce the combinatorial background, additional cuts were imposed on the $K^{*\pm}$ candidates: (1) the kinematical region $x < 0.05$ is excluded from the analysis, because the acceptance drops sharply with decreasing x ; (2) we demand $\cos\theta^* > -0.8$, where θ^* is the pion decay angle in the K_S^0 rest frame. This cut efficiently reduces the

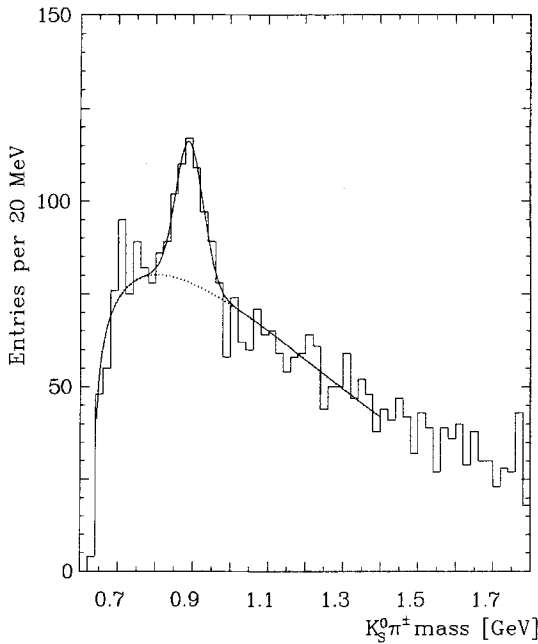


Fig. 3. Invariant $K_S^0 \pi^\pm$ mass spectrum

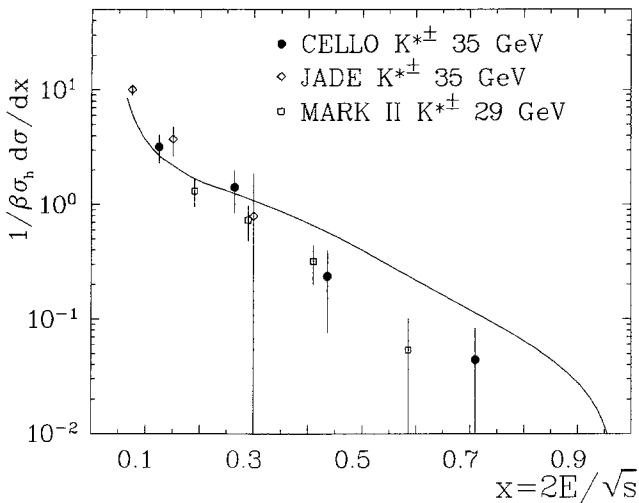


Fig. 4. Scale invariant differential cross section for $K^{*\pm}$ production as a function of the fractional energy $x=2E/\sqrt{s}$. The MARK II and JADE data are taken from [18, 20] and the solid line shows the Lund model prediction

background observed for backward decays. The resulting $K_S^0 \pi^+$ mass distribution is shown in Fig. 3. A prominent $K^{*\pm}$ signal is seen well above threshold. The spectrum is fitted by a Gaussian above a polynomial background function. A fit from threshold to $m(K_S^0 \pi^+) = 1.4 \text{ GeV}/c^2$ gives the following results:

$$m(K^{*+}) = 890 \pm 7 \text{ MeV}/c^2$$

and

$$\sigma(K^{*+}) = 37 \pm 8 \text{ MeV}/c^2.$$

The observed signal is in satisfactory agreement in width and position with that obtained by a Monte Carlo simulation. Following the procedure outlined above for the K_S^0 we determine the inclusive cross section for K^{*+} production corrected for the effect of initial state radiation. The branching ratio for $K^{*+} \rightarrow K_S^0 \pi^+ \rightarrow \pi^+ \pi^- \pi^+$ was taken to be 22.9% [9]. The resulting cross sections are summarized in Table 3 (p. 399) and displayed in Fig. 4 together with the Lund model prediction. The agreement is reasonable, but as is visible in Fig. 4, the combined data from PEP and PETRA indicate a somewhat steeper drop of the cross section with increasing x than suggested by the Lund model. The integrated cross section is $186 \pm 40 \pm 33 \text{ pb}$ for the x range covered by this analysis. Again relying on the Lund model to correct for the unobserved x region, we obtain a total cross section of $214 \pm 46 \pm 39 \text{ pb}$ which translates into an R value of $3.02 \pm 0.65 \pm 0.54$ and implies a mean multiplicity per multihadronic event of $\langle N_{K^{*\pm}} \rangle = 0.77 \pm 0.17 \pm 0.14$. These results are listed in Table 4 and compared to other PEP and PETRA experiments in Table 6, where consistent agreement is found.

3.3 Vector meson production

A comparison of pseudoscalar (P) and vector (V) meson production rates can provide valuable information on the dynamics of quark fragmentation. However, since measured production rates of a certain particle always contain contributions from higher mass states, it is not straightforward to compute the $V/(V+P)_S$ parameter*. Either one needs to know the cross sections and branching ratios of all particles decaying to the observed particle, or one has to rely on a specific fragmentation model. Here we have used the version 6.3 of the Lund model [8] to establish the functional relation between the experimentally accessible ratio $r = N_{K^0, \bar{K}^0}/N_{K^{*\pm}} = 1.84 \pm 0.42 \pm 0.18$ and the V_S parameter for strange quark fragmentation. For this purpose we kept all other Lund model parameters at their default values and varied only the V_S parameter. With a V_S parameter of $0.59^{+0.20+0.10}_{-0.10-0.05}$ the model is in accord with the observed r ratio. The first error is statistical and the second systematic error covers the uncertainties inherent in the measured r ratio. (Note that errors on the absolute normalisation cancel in the ratio r .) With this V_S parameter the model also reproduces the K_S^0 and $K^{*\pm}$ production rates individually with good precision.

Our measurement of V_S compares well with those of JADE [20] ($0.7 \pm 0.35 \pm 0.26$), HRS [25] (0.66 ± 0.08) and TPC [12] ($0.47 \pm 0.11 \pm 0.09$), all based on K^*/K production. The weighted mean of the four results is 0.60 ± 0.06 , to be compared with the value 0.75 expected from spin counting neglecting the mass differences between pseudoscalar and vector mesons. The observed partial suppression of vector meson production can be argued to be due to spin-spin interactions [11] of the

* For brevity $V/(V+P)_S$ is denoted by V_S

quarks forming the meson. According to this description, a mass dependence of the ratio P/V as $\frac{1}{3}(M_V/M_P)^\alpha$ is expected, where α is a free parameter. Combining our data with results from ρ^0/π^0 and D^*/D^0 production leads to $\alpha=0.53\pm 0.16$ [5], in agreement with results obtained by HRS and JADE [19, 20].

4 Analysis of Λ production

The analysis of Λ production follows the same lines as the K_S^0 analysis, but the different decay kinematics and the longer lifetime require somewhat different selection criteria. For V^0 momenta above ≈ 300 MeV/c a unique Λ and $\bar{\Lambda}$ assignment can be made, using the property of the Lorentz transformation, which gives the higher momentum to the more massive decay particle. In the following, reference to the particle state again implies the charge conjugate state as well.

To select Λ candidates we start with the V^0 selection as described in Sect. 3. V^0 candidates compatible with the photon hypothesis were rejected, and the following additional requirements were made: (1) The V^0 momentum must exceed 0.5 GeV/c², below which limit the acceptance drops significantly; (2) the decay length must be larger than 3 cm and (3) r_0 must be larger than 5 mm for the pion and 1 mm for the proton, where r_0 is the closest distance of the track to the beam axis. The $p\pi^-$ effective mass spectrum in Fig. 5 shows a clear Λ signal above a background which is partly ($\approx 30\%$) due to K_S^0 decays into $\pi^+\pi^-$. To avoid further loss of statistics, we have not excluded the K_S^0 reflection explicitly. The spectrum is approximated by a Gaussian signal and a polynomial background function. The fitted background is indicated by the solid line in Fig. 5. The ob-

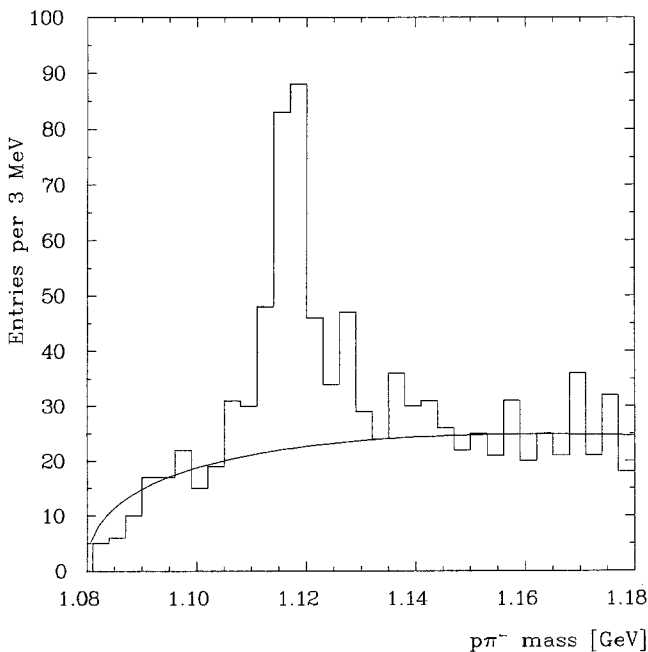


Fig. 5. $p\pi^-/\bar{p}\pi^+$ invariant mass spectrum

served width of 4.5 ± 0.4 MeV/c² is in good agreement with the simulated $p\pi^-$ mass resolution of the detector. The total spectrum contains 220 ± 21 Λ and $\bar{\Lambda}$, where the individual contributions are 107 ± 13 Λ and 110 ± 14 $\bar{\Lambda}$ respectively.

To obtain the differential cross section, the fit was repeated in different x intervals, with width and mass of the signal fixed to the Monte Carlo expectation. The acceptance corrections are determined by running the analysis programs, used for the real data, on a set of Monte Carlo events. The Λ lifetime was computed from the corrected decay length distribution and agrees with the PDG value, thus serving as a test for the correction procedure.

The scale invariant differential cross section, corrected for initial state radiation is presented in Table 5 (p. 400), where the branching ratio $\Lambda\rightarrow p\pi^-$ was taken to be 64.1% [9]. In Fig. 6 the Lund model expectation is shown together with the measured cross section, where good agreement in shape and absolute normalisation is observed.

The analyzed x region corresponds to an integrated cross section of $56.0\pm 7.3\pm 7.3$ pb. The second error is

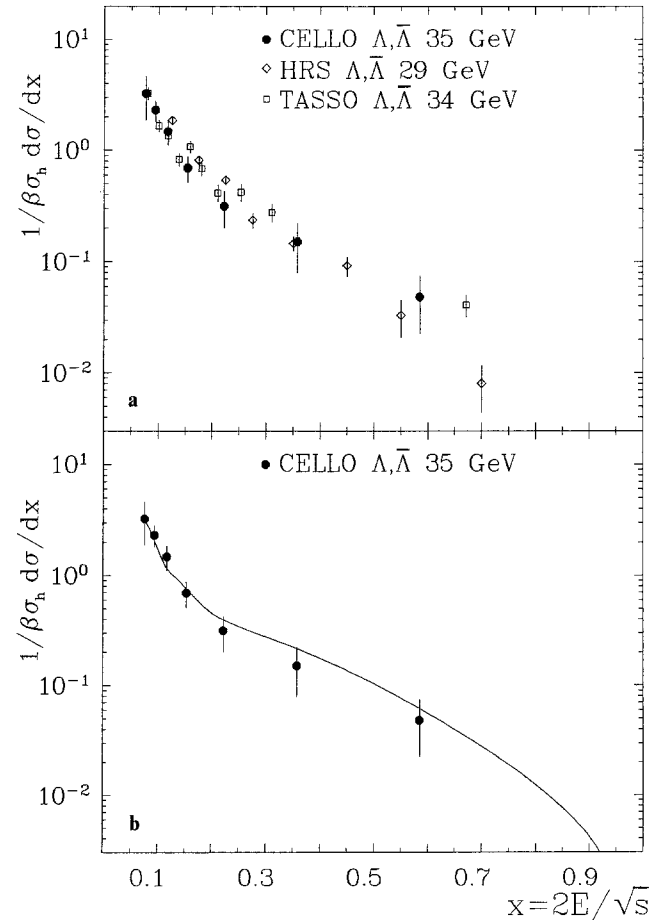


Fig. 6a, b. Scale invariant differential cross section for $\Lambda, \bar{\Lambda}$ production as a function of the fractional energy $x=2E/\sqrt{s}$: a Comparison with other experiments [14, 23]; b comparison with the Lund model prediction

systematic and covers uncertainties in the Monte Carlo simulation, the luminosity and the radiative correction. We use the Lund model to extrapolate over the unmeasured x region and obtain $58.5 \pm 7.6 \pm 7.6$ pb. A comparison with the strange meson yield in Table 4 reveals a significantly lower baryon production rate in the fragmentation process. In Table 6 and Fig. 6 our results are seen to be in agreement with those obtained by other PEP and PETRA collaborations.

5 Summary and conclusions

In a study of strange particles produced inclusively in e^+e^- annihilation, we have measured the production rates for K^0 , \bar{K}^0 , $K^{*\pm}$ and Λ , $\bar{\Lambda}$ and find consistency with results reported by other PEP and PETRA experiments. The data are reproduced with good accuracy by the Lund string model. The ratio of primary pseudoscalar to vector meson production rates, as determined from K_S^0 and $K^{*\pm}$ production, indicates a suppression of the vector meson in the fragmentation process. This behaviour is also suggested by theoretical ideas of quark fragmentation. The strange baryon yield is significantly lower than the strange meson yield, a result also favoured by phenomenological fragmentation models.

Acknowledgements. We gratefully acknowledge the outstanding efforts of the PETRA machine group which made possible these measurements. We are indebted to the DESY computer centre for their excellent support during the experiment. We acknowledge the invaluable effort of the many engineers and technicians from the collaborating institutions in the construction and maintainance of the apparatus. The visiting groups wish to thank the DESY directorate for the support and kind hospitality extended to them. This work was partly supported by the Bundesministerium für Forschung und Technologie (Germany), by the Commissariat à l'Énergie Atomique and the Institut National de Physique Nucléaire et de Physique des Particules (France), by the Istituto Nazionale di Fisica Nucleare (Italy), by the Science and Engineering

Research Council (UK) and by the Ministry of Science and Development (Israel).

References

1. CELLO Coll. H.J. Behrend et al.: DESY 89-008, submitted to Z. Phys. C – Particles and Fields
2. CELLO Coll. H.J. Behrend et al.: Phys. Scr. 23 (1981) 610
3. CELLO Coll. H.J. Behrend et al.: Z. Phys. C – Particles and Fields 44 (1989) 63
4. CELLO Coll. H.J. Behrend et al.: Z. Phys. C – Particles and Fields 42 (1989) 367
5. O. Podobrin: Production of Strange and Charmed Mesons in e^+e^- Annihilation at 35 GeV, Thesis (in German), DESY-F14-88-04 (1988)
6. B. Anderson et al., Phys. Rep. 97 (1983) 33; Z. Phys. C – Particles and Fields 20 (1983) 317; T. Sjöstrand, Comp. Phys. Commun. 27 (1982) 243
7. F.A. Berends, R. Kleiss: Nucl. Phys. B177 (1981) 141
8. T. Sjöstrand et al.: Comp. Phys. Commun. 43 (1987) 367
9. Review of Particle Properties, Particle Data Group: Phys. Lett. 170B (1986)
10. G. D'Agostini, W. de Boer, G. Grindhammer: DESY 89-057, to be published in Phys. Lett. B229 (1989) 160
11. B. Anderson, G. Gustafson, G. Ingelmann, T. Sjöstrand: Phys. Lett. 97C (1983) 31
12. TPC Coll. H. Aihara et al.: Phys. Rev. Lett. 53 (1984) 2378
13. MARK II Coll. H. Schellman et al.: Phys. Rev. D31 (1985) 3013
14. HRS Coll. M. Derrick et al.: Phys. Rev. D35 (1987) 2639
15. PLUTO Coll. Ch. Berger et al.: Phys. Lett. 104B (1981) 79
16. JADE Coll. W. Bartel et al.: Z. Phys. C – Particles and Fields 20 (1983) 187
17. TASSO Coll. M. Althoff et al.: Z. Phys. C – Particles and Fields 27 (1985) 27
18. MARK II Coll. H. Schellman et al.: SLAC Pub. 3448 (1984)
19. HRS Coll. S. Abachi et al.: Phys. Lett. 199B (1987) 151
20. JADE Coll. W. Bartel et al.: Z. Phys. 145B (1984) 441
21. MARK II Coll. C. de la Vaissiere et al.: Phys. Rev. Lett. 54 (1985) 2071
22. TPC Coll. H. Aihara et al.: Phys. Rev. Lett. 54 (1985) 274
23. TASSO Coll. W. Braunschweig et al.: DESY 88-173
24. JADE Coll. W. Bartel et al.: Phys. Lett. 104B (1981) 325
25. HRS Coll. M. Derrick et al.: Phys. Lett. 158B (1985) 519